

# Angular dependence of the bulk nucleation field $H_{c2}$ of aligned $\text{MgB}_2$ crystallites

O. F. de Lima, C. A. Cardoso, R. A. Ribeiro, M. A. Avila & A. A. Coelho

*Instituto de Física "Gleb Wataghin", UNICAMP, 13083-970, Campinas, SP, Brazil*

Studies on the new  $\text{MgB}_2$  superconductor<sup>1</sup>, with a critical temperature  $T_c \approx 39$  K, have evidenced its potential for applications<sup>2,3</sup>, although intense magnetic relaxation effects limit the critical current density,  $J_c$ , at high magnetic fields<sup>4</sup>. This means that effective pinning centers must be added<sup>5</sup> into the material microstructure, in order to halt dissipative flux movements. Concerning the basic microscopic mechanism to explain the superconductivity in  $\text{MgB}_2$ , several experimental<sup>6,7,8,9,10,11,12</sup> and theoretical<sup>13,14,15</sup> works have pointed to the relevance of a phonon-mediated interaction, in the framework of the BCS theory. Questions have been raised about the relevant phonon modes, and the gap and Fermi surface anisotropies, in an effort to interpret spectroscopic and thermal data that give values between 2.4 and 4.5 for the ratio  $2\Delta_0 / kT_c$ , where  $\Delta_0$  is the gap energy and  $k$  is the Boltzmann constant. Preliminary results on the anisotropy of  $H_{c2}$  have shown a ratio, between the in-plane and perpendicular directions, around 1.7 for aligned  $\text{MgB}_2$  crystallites<sup>16</sup> and 1.8 for epitaxial thin films<sup>17</sup>. Here we show a study on the angular dependence of  $H_{c2}$  pointing to a Fermi velocity anisotropy around 2.5. This anisotropy certainly implies the use of texturization techniques to optimize  $J_c$  in  $\text{MgB}_2$  wires and other polycrystalline components.

We measured a sample of well-aligned  $\text{MgB}_2$  crystallites whose preparation details have been described elsewhere<sup>16</sup>. Briefly, a  $\text{MgB}_2$  powder of almost 100% crystallites, having sizes up to  $30 \times 20 \times 5 \mu\text{m}^3$ , was obtained from a weakly sintered material reacted at a temperature  $T = 1200$  °C, much higher than the currently reported values below 900 °C. By spreading this powder on both sides of a paper we aligned the crystallites with their  $ab$  planes sitting on the paper surface. Several samples were then mounted consisting of a pile of five squares of  $3 \times 3 \text{ mm}^2$ , cut from the *crystallite-painted* paper and glued with Araldite resin.

Measurements of the magnetic moment and  $ac$  susceptibility were performed, respectively, with a SQUID magnetometer (model MPMS-5) and a PPMS-9T machine, both made by Quantum Design. In order to obtain the angular dependence under an axial applied field a sample holder was built as sketched in Fig. 1. All parts were machined from a teflon rod, except the removable acrylic protractor, which is about 40 times larger than the hollow box. The  $\text{MgB}_2$  sample (in black) is mounted vertically inside the box that is tightly inserted into a 5 mm diameter hole. This hole is drilled in the plane surface of the sectioned rod that, finally, is attached at the end of the system transport stick. A squared opening was made in the protractor's center such that it fits precisely around the box sides. In this way we are able to rotate the sample with a precision of  $\pm 0.5$  deg, which is good enough in view of the crystallites misalignment, evaluated<sup>16</sup> to be 2.3 deg around the sample  $c$  axis. The

inconvenience of taking the sample holder out of the system, every time that a new angle has to be set, is compensated by its simplicity and small magnetic background.

Fig. 2 shows the magnetic dependence of the magnetization in  $T = 25$  K, for a few representative angles,  $\theta$ , between the sample  $c$  axis and the magnetic field direction. The inset displays a relatively sharp transition with onset at  $T_c = 39$  K, measured with  $H = 10$  Oe in a zero-field cooling (ZFC) and field-cooling measured on cooling (FCC) procedures. The ZFC measurements shown in the main frame look noisy possibly due to the effect of intense vortex creep<sup>4</sup>, combined with a complex regime of flux penetration in the granular sample. The occurrence of random weak links and the varied coupling between grains produce a fluctuating behavior in the sample overall response. However, in all cases we were able to define  $H_{c2}(\theta)$ , at the crossing point between the horizontal baseline and the straight line drawn across the experimental points in the region near the onset of transition. This linear behavior of the magnetization close to the onset is indeed expected from the Ginzburg-Landau (G-L) theory<sup>18</sup>. A constant paramagnetic background was subtracted from all sets of data. In fact one of the reasons for measuring at 25 K is because at this temperature  $H_{c2}(\theta)$  ranges between 28 - 36 kOe, where the paramagnetic background is saturated<sup>16</sup>.

Fig. 3 displays  $H_{c2}(\theta)$  for  $\theta$  between - 20 deg and 120 deg. The vertical error bars were estimated to be around  $\pm 1$  kOe while the horizontal error bars, of  $\pm 2.5$  deg, almost coincide with the symbol size. The solid line going through the experimental points represents a good fit of the angular dependence, predicted by the 3D anisotropic G-L theory to be<sup>18,19</sup>  $H_{c2}(\theta) = H_{c2}^c [\cos^2(\theta) + \varepsilon^2 \sin^2(\theta)]^{-0.5}$ , where  $\varepsilon^2 = m_{ab} / m_c = (H_{c2}^c / H_{c2}^{ab})^2$  is the mass anisotropy ratio and  $H_{c2}^c / H_{c2}^{ab}$  is the ratio between the bulk nucleation field along the  $c$  direction and parallel to the  $ab$  planes. We found  $\varepsilon^2 \approx 0.39 \pm 0.01$ , giving  $H_{c2}^c / H_{c2}^{ab} \approx 0.62$ , which is close to the value of 0.59 anticipated<sup>16</sup> by  $ac$  susceptibility measurements done for the two extreme  $\theta$  positions, at 0 and 90 degrees. Fig. 3 shows also five data points ( $\theta = 0, 25, 65, 85, 90$  deg) marked with stars, which were obtained at the onset of transition of the real part of the complex susceptibility, measured with an excitation field of amplitude 1 Oe and frequency 5 kHz. From  $H_{c2}^{ab} / H_{c2}^c = \xi_{ab} / \xi_c \approx 1.6$ ,  $H_{c2}^c(T) = \Phi_0 / (2\pi \xi_{ab}^2)$ , and using the G-L mean field expression<sup>18</sup> for the coherence length  $\xi(T) = \xi_0 (1 - T/T_c)^{-0.5}$ , we find  $\xi_{0,ab} \approx 65$  and  $\xi_{0,c} \approx 40$ , the coherence length at  $T = 0$  in the  $ab$  planes and along the  $c$  axis, respectively. The quantum of flux, in CGS units, is  $\Phi_0 = 2.07 \times 10^{-7}$  G cm<sup>2</sup>. The ratio  $H_{c2}^{ab} / H_{c2}^c \approx 1.6$  reminds the relationship predicted for the surface nucleation field<sup>20</sup>  $H_{c3} \approx 1.7 H_{c2}$ . However, this is clearly not the case of our data, as one can see from the expected angular dependence of  $H_{c3}(\theta)$  for thick samples<sup>21</sup>, which is plotted in Fig. 3 as a dash-dotted curve. The dashed curve in between represents the well-known Thinkham's formula<sup>22</sup> for the surface nucleation field in very thin films. Therefore, a characteristic feature of the surface nucleation field is the cusplike curve shape near  $\theta = 90$  deg, which contrasts with the sinusoidal shape followed by our data.

The  $H_{c2}$  anisotropy can be caused by an anisotropic gap energy or by an anisotropic Fermi surface, as well as by a combination of both effects<sup>23</sup>. Assuming an isotropic gap one gets  $\xi_{ab} / \xi_c = V_F^{ab} / V_F^c$ , implying for our data  $V_F^{ab} \approx 1.6 V_F^c$ , for the Fermi velocities within

the  $ab$  plane and along the  $c$  direction. However, several experimental<sup>8,10,11</sup> and theoretical<sup>13,14,15</sup> works have suggested an anisotropic gap energy for MgB<sub>2</sub>. In particular, two recent reports<sup>11,15</sup> rely on the analysis of spectroscopic and thermodynamic data to propose an anisotropic s-wave pairing symmetry, such that the minimum gap value,  $\Delta_0 \approx 1.2 kT_c$ , occurs within the  $ab$  plane. Using this result and assuming an isotropic Fermi surface the expected  $H_{c2}$  anisotropy would be<sup>15</sup>  $H_{c2}^{ab} / H_{c2}^c \approx 0.8$ . This conflicts with our present findings and with other results<sup>16,17</sup> that show clearly  $H_{c2}^{ab} > H_{c2}^c$ . However, by allowing a Fermi surface anisotropy in their model, Haas and Maki have found that<sup>24</sup>  $V_F^{ab} \approx 2.5 V_F^c$  in order to match our result of  $H_{c2}^{ab} / H_{c2}^c \approx 1.6$ , at  $T = 25$  K. Therefore the two fundamental sources of microscopic anisotropy affects the  $H_{c2}$  anisotropy of MgB<sub>2</sub> in opposite ways. As a consequence of combining both effects to explain the  $H_{c2}$  anisotropy, the Fermi velocity anisotropy becomes about 60% higher when compared with the isotropic gap hypothesis. Interestingly, a calculation based on a two-band model has also found<sup>25</sup>  $V_F^{ab} \approx 2.5 V_F^c$ , while a much smaller value of  $V_F^{ab} \approx 1.03 V_F^c$  was found in a band structure calculation using a general potential method<sup>13</sup>.

Concluding, the  $H_{c2}$  anisotropy ratio for MgB<sub>2</sub> implies an anisotropy of the Fermi velocity of at least  $V_F^{ab} \approx 1.6 V_F^c$ , for an isotropic gap hypothesis. In a more realistic scenario of an s-wave anisotropic gap this ratio could increase to  $V_F^{ab} \approx 2.5 V_F^c$ . Finally, since  $J_c$  is proportional to  $\xi^2$ , it is worth noticing that<sup>26</sup>  $J_c(H // c) / J_c(H // ab) \approx \xi_{ab} / \xi_c \approx H_{c2}^{ab} / H_{c2}^c$ . Therefore we anticipate that the in-plane critical current density values are expected to be about 60% higher than the values along the  $c$  direction ( $H // ab$ ). Indeed this  $J_c$  anisotropy could be even higher as observed in thin films<sup>17</sup>. This means that in order to optimize  $J_c$  in wires or other polycrystalline components some texturization technique will be useful.

---

## REFERENCES

- <sup>1</sup> Nagamatsu, J., Nakagawa, N., Muranaka, T., Zenitani Y. & Akimitsu, J. Superconductivity at 39 K in magnesium diboride. *Nature* **410**, 63-64 (2001).
- <sup>2</sup> Larbalestier, D. C. *et al.* Strongly linked current flow in polycrystalline forms of the superconductor MgB<sub>2</sub>. *Nature* **410**, 186-189 (2001).
- <sup>3</sup> P. C. Canfield *et al.* Superconductivity in Dense MgB<sub>2</sub> Wires. *Phys. Rev. Lett.* **86**, 2423-2426 (2001).
- <sup>4</sup> Bugoslavski, Y., Perkins, G. K., Qi, X., Cohen, L. F. & Caplin A. D. Vortex dynamics in superconducting MgB<sub>2</sub> and prospects for applications. *Nature* **410**, 563-565 (2001).
- <sup>5</sup> Bugoslavski, Y. *et al.* Enhancement of the high-field critical current density of superconducting MgB<sub>2</sub> by proton irradiation. *Nature* (in the press).
- <sup>6</sup> Bud'ko, S. L. *et al.* Boron isotope effect in superconducting MgB<sub>2</sub>. *Phys. Rev. Lett.* **86**, 1877-1880 (2001).
- <sup>7</sup> Karapetrov, G., Iavarone, M., Kwok, W. K., Crabtree, G. W. & Hinks, D. G. Scanning tunneling spectroscopy in MgB<sub>2</sub>. *Phys. Rev. Lett.* **86**, 4374-4377 (2001).
- <sup>8</sup> Wang, Y., Plackowski T. & Junod, A. Specific heat in the superconducting and normal state (2-300 K, 0-16 Teslas), and magnetic susceptibility of the 38 K superconductor MgB<sub>2</sub>: evidence for a multicomponent gap. Preprint cond-mat/0103181 at <<http://xxx.lanl.gov>> (2001).
- <sup>9</sup> Yildirim, T. *et al.* Giant anharmonicity and non-linear electron-phonon coupling in MgB<sub>2</sub>: A combined first-principles calculations and neutron scattering study. *Phys. Rev. Lett.* (in the press).
- <sup>10</sup> Bouquet, F., Fisher, R. A., Philips, N. E., Hinks, D. G. & Jorgensen J. D. Specific Heat of Mg<sup>11</sup>B<sub>2</sub>. Preprint cond-mat/0104206 at <<http://xxx.lanl.gov>> (2001).

- <sup>11</sup> Chen, C.-T. *et al.* Spectroscopic evidence for anisotropic s-wave pairing symmetry in MgB<sub>2</sub>. Preprint cond-mat/0104285 at <http://xxx.lanl.gov> (2001).
- <sup>12</sup> Martinho, H. *et al.* Evidence for resonant behavior of the E<sub>2g</sub> phonon in MgB<sub>2</sub>. Preprint cond-mat/0105204 v2 at <http://xxx.lanl.gov> (2001).
- <sup>13</sup> Kortus, J., Mazin I. I., Belashchenko, K. D., Antropov V. P. & Boyer L. L. Superconductivity of metallic boron in MgB<sub>2</sub>. *Phys. Rev. Lett.* **86**, 4656-4659 (2001).
- <sup>14</sup> An, J. M. & Pickett, W. E. Superconductivity of MgB<sub>2</sub>: covalent bonds driven metallic. Preprint cond-mat/0102391 v2 at <http://xxx.lanl.gov> (2001).
- <sup>15</sup> Haas, S. & Maki, K. Anisotropic s-wave superconductivity in MgB<sub>2</sub>. Preprint cond-mat/0104207 at
- <sup>16</sup> de Lima, O. F., Ribeiro, R. A., Avila, M. A., Cardoso, C. A. & Coelho A.A. Anisotropic superconducting properties of aligned MgB<sub>2</sub> crystallites. *Phys. Rev. Lett.* (in the press).
- <sup>17</sup> Patnaik, S. *et al.* Electronic anisotropy, magnetic field-temperature phase diagram and their dependence on resistivity in c-axis oriented MgB<sub>2</sub> thin films. Preprint cond-mat/0104562 at
- <sup>18</sup> Tinkham, M. *Introduction to superconductivity*, 2<sup>nd</sup> ed. (McGraw-Hill, New York, 1996).
- <sup>19</sup> Tilley, D. R. The Ginzburg-Landau equations for anisotropic alloys. *Proc. Phys. Soc. London* **86**, 289-295 (1965).
- <sup>20</sup> Saint-James, D. & de Gennes, P. G. Onset of superconductivity in decreasing fields. *Physics Letters* **7**, 306-308 (1963).
- <sup>21</sup> Yamafuji, K., Kusayanagi, E., & Irie, F. On the angular dependence of the surface superconducting critical field. *Physics Letters* **21**, 11-13 (1966).
- <sup>22</sup> Tinkham M. Angular dependence of the superconducting nucleation field. *Physics Letters* **9**, 217-218 (1964).
- <sup>23</sup> Weber, H. W. (ed) *Anisotropy Effects in Superconductors* (Plenum Press, New York, 1977).
- <sup>24</sup> Haas, S. private communications.
- <sup>25</sup> Shulga, S. V., Drechsler S. -L., Eschrig, H., Rosner, H. & Pickett W. E. The upper critical field problem in MgB<sub>2</sub>. Preprint cond-mat/0103154 at <http://xxx.lanl.gov> (2001).
- <sup>26</sup> Blatter, G., Feigel'man, M. V., Geshkenbein, V. B., Larkin, A. I. & Vinokur V. M. Vortices in high-temperature superconductors. *Rev. Mod. Phys.* **66**, 1125-1388 (1994).

#### Acknowledgements

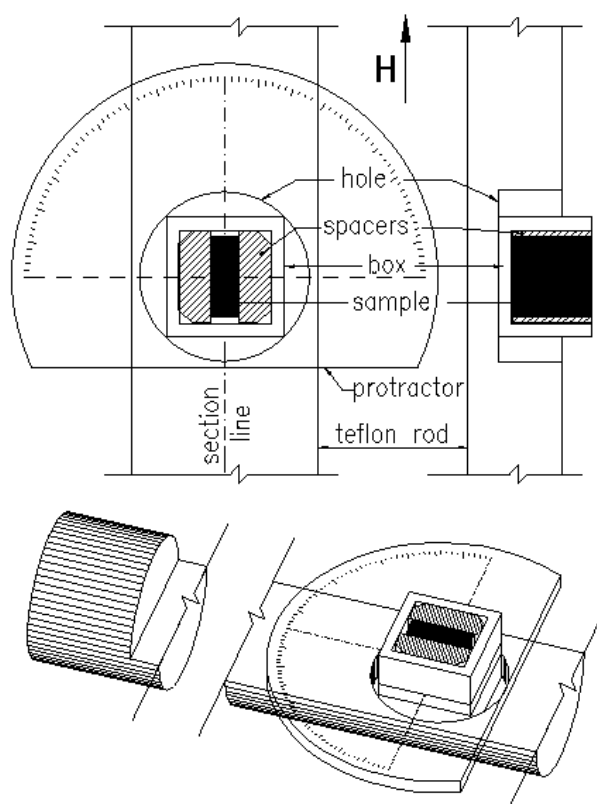
We thank S. Haas, A. V. Narlikar and O. P. Ferreira for useful discussions and acknowledge the financial support from the Brazilian Science Agencies FAPESP and CNPq.

**Correspondence and requests for materials should be addressed to O.F. de Lima (delima@ifi.unicamp.br).**

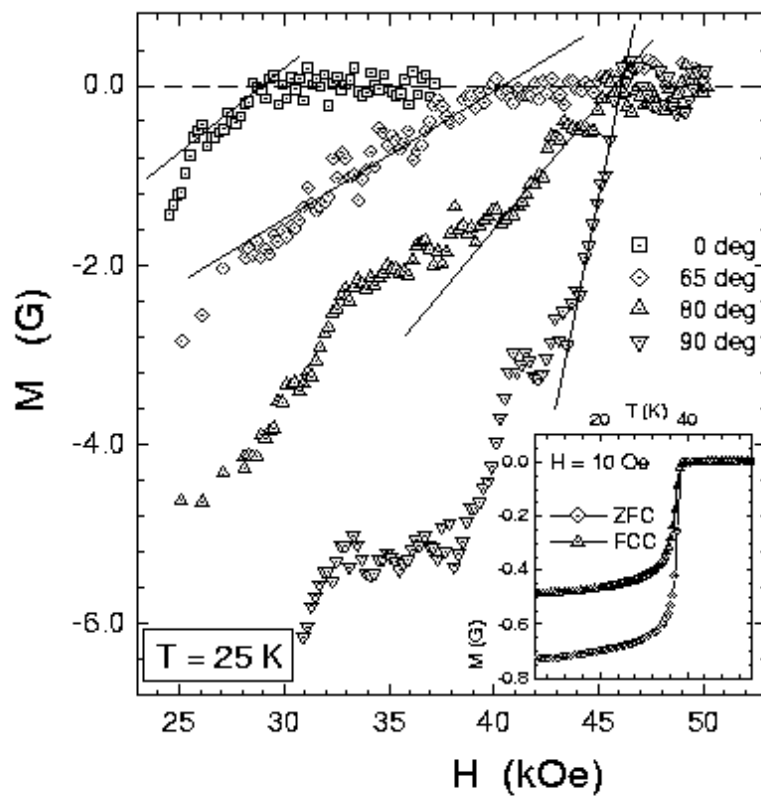
Figure 1 Sketch of the sample holder used to get the angular dependence of the sample magnetization in a SQUID magnetometer. The sample (in black) is inside the hollow box, that is tightly inserted into a 5 mm diameter hole. The removable acrylic protractor fits precisely around the box in order to indicate the angular position.

Figure 2 Zero Field Cooling magnetization measurements as a function of the applied field, for  $\theta = 0, 65, 80, 90$  degrees. The bulk nucleation field  $H_{c2}(\theta)$  is defined at the crossing of the auxiliary straight lines and the horizontal baseline ( $M = 0$ ). The inset shows ZFC and FCC magnetization measurements as a function of temperature for  $H = 10$  Oe, giving  $T_c \approx 39$  K.

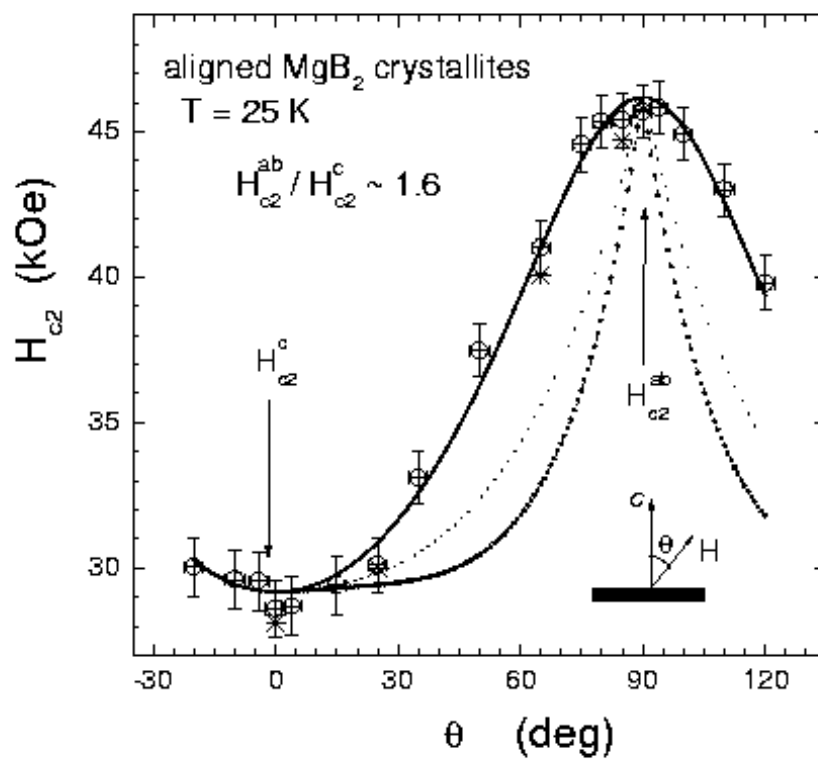
Figure 3 Bulk nucleation field (or upper critical field),  $H_{c2}$ , as a function of the angle,  $\theta$ , between the sample c axis and the magnetic field direction. Plots of the expected angular dependence for the surface nucleation field,  $H_{c3}$ , in thick samples (dash-dotted curve) and very thin films (dashed curve) are also shown. The stars at  $\theta = 0, 25, 65, 85, 90$  degrees represent  $H_{c2}(\theta)$  obtained at the onset of transition of the real part of  $ac$  susceptibility measurements.



de Lima et al. - Fig. 1



de Lima et al. - Fig. 2



de Lima et al. - Fig. 3